Complex interaction network revealed by mutation of human telomerase 'insertion in fingers' and essential N-terminal domains and the telomere protein TPP1

Received for publication, September 8, 2022, and in revised form, January 5, 2023 Published, Papers in Press, January 14, 2023,
https://doi.org/10.1016/j.jbc.2023.102916

Patrick Lambert-Lanteigne[1], **Adrian Young**[1,2], **and Chantal Autexier**[1,2,3,*]

From the [1]*Lady Davis Institute for Medical Research, Jewish General Hospital, Montréal, Canada;* [2]*Department of Anatomy and Cell Biology, and* [3]*Department of Medicine, McGill University, Montréal, Canada*

Reviewed by members of the JBC Editorial Board. Edited by Patrick Sung

In the majority of human cancer cells, cellular immortalization depends on the maintenance of telomere length by telomerase. An essential step required for telomerase function is its recruitment to telomeres, which is regulated by the interaction of the telomere protein, TPP1, with the telomerase essential N-terminal (TEN) domain of the human telomerase reverse transcriptase, hTERT. We previously reported that the hTERT 'insertion in fingers domain' (IFD) recruits telomerase to telomeres in a TPP1-dependent manner. Here, we use hTERT truncations and the IFD domain containing mutations in conserved residues or premature aging disease-associated mutations to map the interactions between the IFD and TPP1. We find that the hTERT-IFD domain can interact with TPP1. However, deletion of the IFD motif in hTERT lacking the N-terminus and the C-terminal extension does not abolish interaction with TPP1, suggesting the IFD is not essential for hTERT interaction with TPP1. Several conserved residues in the central IFD-TRAP region that we reported regulate telomerase recruitment to telomeres, and cell immortalization compromise interaction of the hTERT-IFD domain with TPP1 when mutated. Using a similar approach, we find that the IFD domain interacts with the TEN domain but is not essential for intramolecular hTERT interactions with the TEN domain. IFD–TEN interactions are not disrupted by multiple amino acid changes in the IFD or TEN, thus highlighting a complex regulation of IFD–TEN interactions as suggested by recent cryo-EM structures of human telomerase.

Telomere maintenance is essential for the replicative immortality characteristic of cancer cells (1). Moreover, defective telomere maintenance due to mutations in telomerase or telomere proteins is characteristic of a collection of Mendelian disorders, referred to as telomeropathies, including the premature aging syndrome, dyskeratosis congenita (2–4). Telomeres are maintained by telomerase, a ribonucleoprotein with reverse transcriptase (RT) activity that minimally consists of a core catalytic subunit, hTERT (human telomerase RT), and an integral RNA component, hTR (human telomerase RNA) that provides the template for telomere synthesis (5, 6). hTERT expression is tightly regulated at the transcriptional level (1). However, one essential step required for telomerase function is its recruitment and activation at the telomere (7). Identifying the mechanisms regulating telomerase recruitment to telomeres will help to uncover novel potential targets for the treatment of cancers and telomeropathies.

Telomerase recruitment to telomeres is regulated by the interaction of the telomere shelterin protein, TPP1, with the telomerase essential N-terminal (TEN) domain of hTERT (8–10). Human TEN and the hTERT 'insertion in fingers domain' (IFD) regulate the unique property of telomerase to repeatedly synthesize the short G-rich telomere repeats using hTR as a template without dissociating from the DNA substrate (11–13). The IFD is located between RT motifs A and B′ and consists of two helices (a and c) and a central region identified as IFDb consisting of three β-sheets later named IFD-TRAP (14, 15). We and others reported that IFD recruits telomerase to telomeres in a TPP1-dependent manner (11, 16). The result of these latter studies and another similar study from our group, examining premature aging disease-associated hTERT variants located in the IFD motif, were suggestive of an indirect or direct interaction of the IFD with TPP1 (17). In support for a TPP1-dependent role of the IFD in telomerase recruitment, cryo-EM structures of *Tetrahymena* telomerase revealed interactions between the TPP1 paralog, p50, and the IFD (14, 18) and interestingly also showed interactions between the TEN domain and the IFD-TRAP for the first time (14). How TPP1 and the hTERT TEN and IFD domains intersect to regulate telomerase recruitment to telomeres and cell immortalization is unknown. Moreover, a structural homology-based mutagenesis screen focused on surface residues of the TEN, and IFD regions identified hTERT residues that are critical for contacting TPP1 but dispensable for other aspects of telomerase structure or function (16). In this latter study, hTERT-TPP1 contacts and binding were inferred based on TEN and IFD-TRAP mutants specifically defective in telomerase recruitment and stimulation by human TPP1.

In the present study, we expressed truncated hTERT enzymes and domains containing mutations in conserved residues or premature aging disease-associated mutations within IFD to map the interactions between the IFD, TEN, and

* For correspondence: Chantal Autexier, chantal.autexier@mcgill.ca.

TPP1 and relate the role of these interactions in the recruitment of telomerase to telomeres and cell immortalization. We found that hTERT lacking the TEN domain and the C-terminal extension (hTERTΔTENΔCTE) can immunoprecipitate TPP1 and TEN. We show that the IFD fragment alone can also coimmunoprecipitate TPP1 and TEN, suggesting that the IFD can interact with TPP1 and TEN. However, deletion of the IFD motif in hTERTΔTENΔCTE does not abolish interaction with TPP1 or TEN, suggesting that the IFD is not essential for the interaction of hTERT with TPP1 or TEN. Several residues in the IFD region that we reported regulate telomerase recruitment to telomeres, and cell immortalization also compromise interaction of the IFD domain with TPP1, when mutated. We further characterized IFD and TEN interactions revealed in recent human telomerase cryo-EM structures (19–22). However, IFD-TEN interactions are not disrupted by multiple amino acid substitutions predicted to disrupt those interactions, highlighting the complex regulation of IFD–TEN interactions.

Results and discussion

The IFD domain interacts with TPP1 but is not essential for the interaction of hTERT with TPP1

Several hTERT regions are known to interact with TPP1 and/or DNA to mediate telomerase recruitment, including the TEN domain and the C-terminal extension (CTE) (8–10, 23, 24). To reveal a possibly weaker TPP1–IFD interaction independent of the TEN or C-terminus, we first generated hTERT deletion variants lacking N-terminal residues 1-316 that comprise the TEN domain (residues 1-200) (25) and linker between TEN and the RNA-binding domain, TRBD (thereafter referred to as ΔTEN) or lacking both the N-terminus and C-terminal residues 936-1132 (ΔTENΔCTE) (Fig. 1*A*). We also created a variant consisting of the hTERT-IFD region alone (residues 721-814). The deletion variants were fused in frame to a FLAG epitope and c-myc nuclear localization signal (NLS). To gain insight into the possible folding of the IFD domain alone, we used an AlphaFold prediction (26–29). Folding of the IFD domain alone predicted by AlphaFold was similar to the structures revealed by cryo-EM (Fig. 1*B*), and inclusion of the FLAG and NLS did not change the predicted IFD structure (not shown). We coexpressed the FLAG-tagged hTERT deletion variants along with C-terminally HA-tagged TPP1 (TPP1-HA) in HEK293 cells and confirmed by Western blotting analysis that TPP1 was expressed and that all the hTERT variants were expressed at the expected molecular weights (Fig. 1*C*) and localized to the nucleus (Fig. 1*D*). To note, we have previously demonstrated that transient transfection of FLAG-tagged hTERT leads to levels of expression above low endogenous hTERT levels, as exogenously expressed hTERT, but not endogenous hTERT, can be detected by Western blot using an anti-hTERT antibody (11).

We found that immunoprecipitation (IP) of full length (FL) FLAG-hTERT WT and FLAG-hTERTΔTEN coimmunoprecipitated coexpressed TPP1-HA, consistent with a previous study reporting that interaction of telomerase with TPP1 is not abolished upon TEN domain deletion (8). We also observed co-IP of TPP1-HA with FLAG-hTERTΔTENΔCTE that contains the IFD domain and with the FLAG-hTERT-IFD region alone, suggesting that the IFD interacts with TPP1, in support of a TPP1-dependent role of the IFD in telomerase recruitment and cryo-EM structures of *Tetrahymena* and human telomerase (11, 14, 17, 18, 20, 21). However, FLAG-hTERTΔTENΔCTE also lacking the IFD domain (ΔTENΔCTEΔIFD) (Fig. 1*A*) was still able to coimmunoprecipitate TPP1-HA (Fig. 1*E*), suggesting that the IFD is not essential for the interaction with TPP1. In addition, these results imply that there may be additional contacts between hTERT and TPP1 that fall outside of the TEN and IFD domains, consistent with results from other studies (9, 10).

IFD-TRAP variants, but not the IFDa or IFDc variants, are compromised in interactions with TPP1 that correlate with severe or TPP1-dependent telomere recruitment and cell immortalization phenotypes

Our previous findings suggesting a TPP1-dependent role for the IFD domain in telomerase recruitment to telomeres were based on the analysis of hTERT variants mutated in conserved and disease-associated residues within the IFDa (P721R, T726M), IFD-TRAP (V763S, P785L, V791Y), or IFDc (L805A, R811C) regions (11, 17, 30) (Fig. 2*A*). In addition to enzyme activity and processivity of these variants, we previously analyzed their localization to telomeres by hTR-fluorescence *in-situ* hybridization in the absence or presence of TPP1 and POT1. Additionally, we analyzed cell growth, short telomeres (signal-free ends), telomeric DNA damage, and immortalization in limited lifespan cells (11, 17). We observed a number of defects for hTERT IFD variants, including the inability to immortalize limited lifespan cells (hTERT-V791Y), and impaired telomere association, which could be partially rescued by TPP1-POT1 overexpression (hTERT-L805A) (11, 30). To better understand if the observed defects correlate with altered IFD–TPP1 interactions, we introduced mutations in these conserved and disease-associated IFD residues in the hTERTΔTENΔCTE variant. We coexpressed the FLAG-hTERTΔTENΔCTE IFD variants along with TPP1-HA in HEK293 cells and confirmed by Western blotting analysis that TPP1-HA and all the hTERT variants were expressed (Fig. 2*B*). However, we found that most of the FLAG-hTERT ΔTENΔCTE IFD WT and variants could similarly coimmunoprecipitate coexpressed TPP1-HA (Fig. 2, *B* and *C*), suggesting compensating binding sites elsewhere on that truncation in accordance with our results with hTERT ΔTENΔCTEΔIFD or that certain single amino acid changes are not sufficient to disrupt the interaction between the IFD and TPP1. However, we observed reduced interaction of TPP1-HA with FLAG-hTERT ΔTENΔCTE-containing mutations V763S and P785L (Fig. 2*C*).

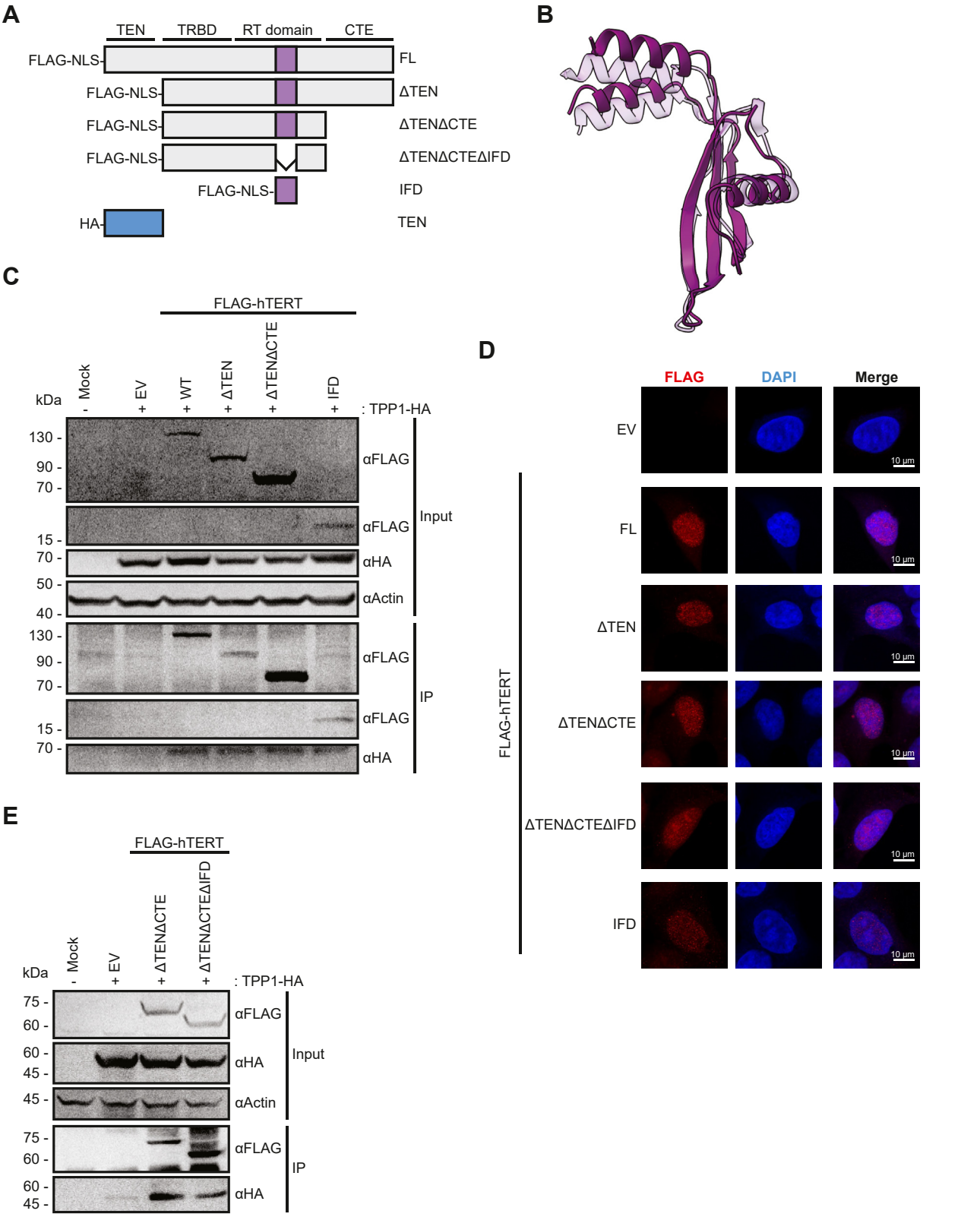

Figure 1. The IFD domain interacts with TPP1 but is not essential for the interaction of hTERT with TPP1. *A*, domain organization of full-length (FL) hTERT with characteristic domains: telomerase essential N-terminal domain (TEN), telomerase RNA–binding domain (TRBD), reverse transcriptase domain (RT) containing the insertion in fingers domain (IFD) in *purple*, and the C-terminal extension (CTE). Engineered deletion constructs are indicated below the full-length WT hTERT. All constructs were created to include FLAG and NLS sequences at the N-terminus. An N-terminally HA-tagged TEN domain containing an endogenous NLS is also depicted in *blue*. *B*, Alphafold (Colabfold) structural prediction of the isolated hTERT sequence (IFD: 721-815) (Solid opacity) compared to the cryo-EM structure of hTERT telomerase IFD from the PBD ID 7BG9 (low opacity). *C*, interactions of FLAG-hTERT WT and the indicated deletion variants with TPP1-HA were assessed by coimmunoprecipitation from HEK293 cell lysates using an anti-FLAG antibody. Representative immunoblots showing input FLAG-hTERT WT and variants and TPP1-HA, and immunoprecipitation of FLAG-hTERT variants and TPP1-HA. Blots were probed using

Based on our results demonstrating that the IFD region alone can interact with TPP1 (Fig. 1*C*), we then introduced the above mutations in the conserved and disease-associated residues in the hTERT IFD fragment, anticipating that alterations in binding of IFD variants with TPP1 might be more easily revealed using this IFD fragment. We coexpressed the FLAG-hTERT IFD variants along with TPP1-HA in HEK293 cells and confirmed by Western blotting analysis that TPP1-HA and all the hTERT variants were expressed (Fig. 2*D*). In the context of the IFD fragment, we observed reduced interaction of TPP1-HA with several IFD variants, including hTERT-IFD V763S, P785L, V791Y, and L805A, but WT or near WT levels of coimmunoprecipitated TPP1-HA for hTERT-IFD variants P721R, T726M and R811C (Fig. 2, *D* and *E*). All the variants with substantial reduction in the levels of coimmunoprecipitated TPP1 are located in the IFD-TRAP region, except for L805A, which is located in the IFDc region near the IFD-TRAP region. These results are consistent with *Tetrahymena* telomerase cryo-EM studies which revealed that the TPP1 paralog p50 interacts with the IFD-TRAP possibly stabilizing the IFD-TRAP fold (14), and IF-FISH studies showing that the addition of human IFD-TRAP to human TEN in a mouse TERT backbone leads to an improvement of telomerase recruitment to human TPP1 comparable to that observed in hTERT-reconstituted telomerase (16). Importantly, due to levels of exogenous hTERT variants greater than endogenous levels, the existence of hTERT as a monomer and the results that some IFD-TRAP mutants are defective in interactions with TPP1, it is unlikely that the lack of interaction defects between certain hTERT variants and TPP1 examined in Figures 1 and 2 are due to interactions being bridged by endogenous hTERT or TPP1.

These results are also consistent with our functional studies where alterations in residues in the IFD-TRAP region (V763S, P785L, V791Y) or flanking the IFD-TRAP region (L805A) lead to more severe and/or TPP1-dependent phenotypes than alterations in other tested residues in the IFDa or IFDc regions (P721R, T726M, and R811C) (11, 17, 30). For example, hTERT V791Y could not immortalize limited lifespan cells, be recruited to telomeres or elongate telomeres when overexpressed in HeLa cells, possibly due to a defect in binding TPP1 (11, 30) (Fig. 2, *D* and *E*). hTERT-L805A had impaired telomere association which could be partially rescued by TPP1-POT1 overexpression, suggesting that excess TPP1 can possibly compensate for defects in TPP1 binding (11). Interestingly, despite growth defects in limited lifespan cells and accumulation of short telomeres and telomere DNA damage, hTERT-V763S could be recruited to telomeres (11), but our current results suggests that mutating this residue interferes with TPP1 binding. Further analysis of this residue will be necessary to understand its function and relationship with TPP1. Lastly, hTERT-P785L's enzyme activity and recruitment to telomeres were stimulated by TPP1-POT1 overexpression, though cells expressing this variant did not display growth defects or telomeric DNA damage in limited lifespan cells (17). Of note, however, recent cryo-EM structures of human telomerase revealed that V763, P785, V791, and L805 are not directly interacting with TPP1 but rather facing away from TPP1 (20, 21) (Fig. 2*F*), suggesting that effects of mutating these residues may indirectly contribute to a defect in TPP1–IFD interactions. It is also important to consider the potential contributions of the missing domains of TPP1 in the currently available structures to the interactions between IFD and TPP1. Of importance, V791 is part of a highly conserved 790VVIE793 motif within the IFD β-sheet–TEN β-sheet interface (β18 in IFD-TRAP and β6 in TEN) and close to TEN and IFD residues that bind to DNA and are implicated in anchor site function. A protein-based anchor site was proposed in the early 1990's to rationalize the repeated addition of telomeric sequences by telomerase on the same DNA substrate without dissociation of telomerase from the DNA during RNA-DNA unpairing (repeat addition processivity), and the TEN domain was later identified as the anchor site (31–36). TPP1 and POT1 help to stabilize the TEN domain and the DNA–TEN interaction that constitute the anchor site, and alterations of V791 could be impacting the regulation of the anchor site by TPP1 and POT1. Interestingly, both V763 and L805 are in proximity to motif 3 within a hydrophobic patch. Motif 3 regulates repeat addition processivity and influences template conformation (15, 37). Importantly, the DNA path to the active site and the RNA-DNA duplex link a number of TERT domains, including TEN, IFD, CTE, and motif 3 (20–22), and alterations in V763 and L805 could impact the coordinated roles of motif 3, IFD, and CTE to facilitate binding of the RNA-DNA duplex during template translocation that was initially proposed by Xie et al. (15).

hTERT-IFD variants P721R, T726M, and R811C, which contain patient-associated mutations in the IFDa and IFDc, coimmunoprecipitate similar levels of TPP1-HA as WT hTERT-IFD. These results are consistent with the recent cryo-EM structures of human telomerase with TPP1 and POT1, in which these residues are located far from TPP1. In our functional studies, alterations at these residues in FL hTERT led to a variety of mild defects in telomerase activity, processivity, and telomere association that could not be rescued by TPP1 (17), and coupled with results from the current study, is consistent with a possible TPP1-independent function of these

antibodies against FLAG or HA or the loading control actin (in the input). EV represents HEK293 cells expressing TPP1-HA but transfected with an empty vector not expressing any hTERT variant. Mock represents untransfected HEK293 cells expressing neither hTERT nor TPP1. n = 4. *D*, full length FLAG-hTERT WT (FL) and the indicated deletion variants or IFD fragment were expressed in HEK293 cells, and localization was assessed in fixed cells by indirect immunofluorescence. Images were acquired using Infinity Capture software and camera (40×; Leica DM2000 fluorescence microscope; Lumenera). The nucleus is indicated by DAPI staining. Nuclear localization of all the variants was confirmed by colocalization of FLAG with DAPI signals (merge). *E*, interactions of FLAG-hTERTΔTENΔCTE and FLAG-hTERTΔTENΔCTEΔIFD with TPP1-HA were assessed by coimmunoprecipitation from HEK293 cell lysates using an anti-FLAG antibody. Representative immunoblots showing input FLAG-hTERTΔTENΔCTE, FLAG-hTERTΔTENΔCTEΔIFD, and TPP1-HA, and immunoprecipitation of FLAG-hTERTΔTENΔCTE, FLAG-hTERTΔTENΔCTEΔIFD, and TPP1-HA. Blots were probed using antibodies against FLAG or HA or the loading control actin (in the input). EV represents HEK293 cells expressing TPP1-HA but transfected with an empty vector not expressing hTERT. Mock represents untransfected HEK293 cells expressing neither hTERT nor TPP1. n = 2. hTERT, human telomerase RT; NLS, nuclear localization signal.

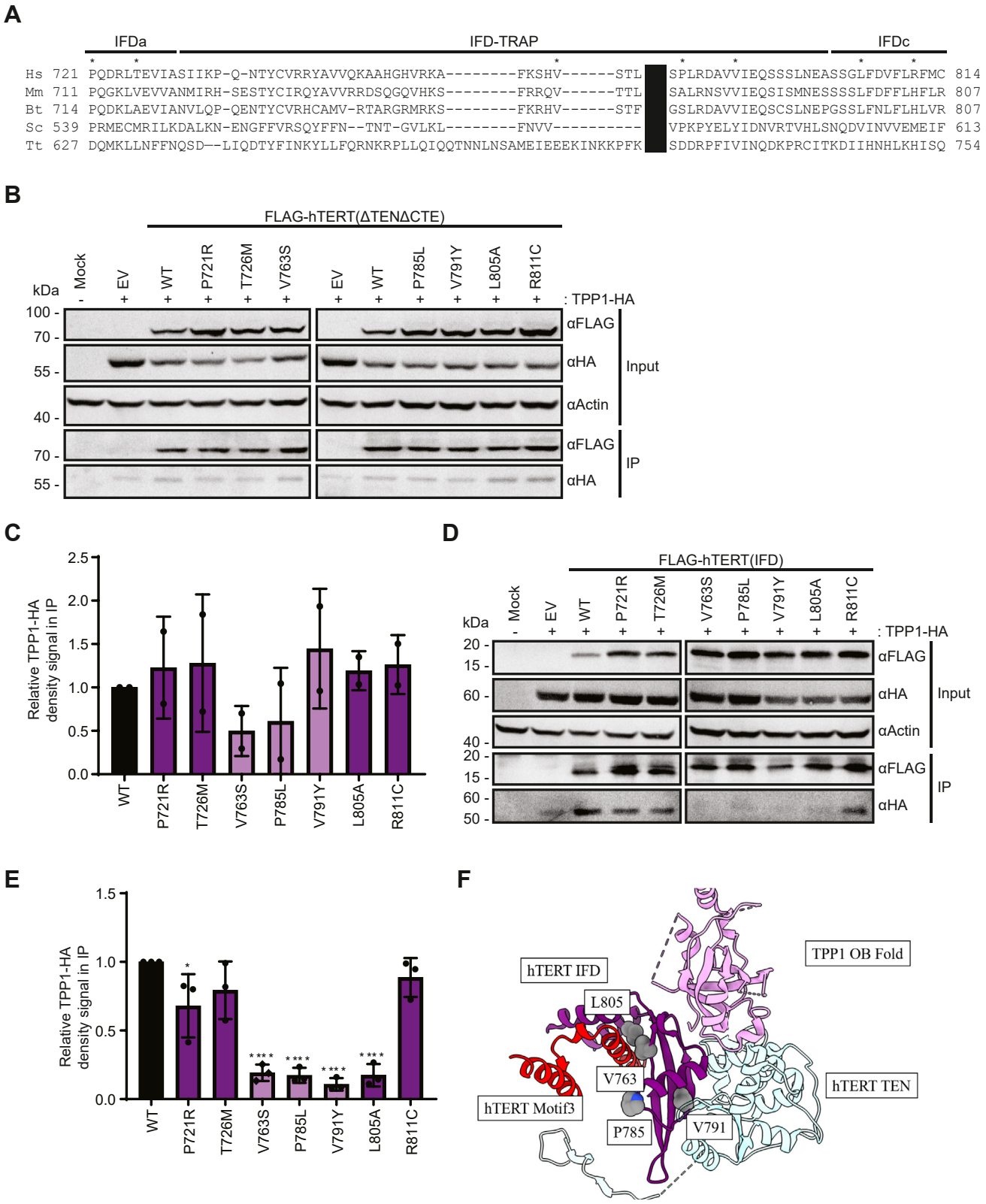

Figure 2. IFD-TRAP variants, but not the IFDa or IFDc variants, are compromised in interactions with TPP1. *A*, sequence alignment of TERT IFDs from selected organisms, *Homo sapiens* (Hs), *Mus musculus* (Mm), *Bos taurus* (Bt), *Saccharomyces cerevisiae* (Sc), *Tetrahymena thermophila* (Tt) was performed using Clustal W2. Labels above the alignment indicate the conserved and disease-associated residues P721, T726, V763, P785, V791, L805, and R811 located in the IFDa, IFD-TRAP, or IFDc, and the corresponding residues at equivalent positions with the other TERTs. Human TERT residues 767-783 and equivalent residues in other organisms are not included in the alignment and are shown as a *black vertical bar*. *B*, interactions of FLAG-hTERTΔTENΔCTE and the indicated IFD variants within FLAG-hTERTΔTENΔCTE with TPP1-HA were assessed by coimmunoprecipitation from HEK293 cell lysates using an anti-FLAG antibody. Representative immunoblots showing input FLAG-hTERTΔTENΔCTE, the indicated IFD variants and TPP1-HA, and immunoprecipitation of FLAG-hTERT variants and TPP1-HA. Blots were probed using antibodies against FLAG or HA or the loading control actin (in the input). EV represents HEK293 cells

residues. Nonetheless, limited lifespan cells expressing these disease-associated hTERT IFD variants displayed mild growth defects and higher levels of apoptosis, short telomeres, and telomere DNA damage compared to cells expressing WT hTERT. Defects may result from effects on interactions between paired IFD residues (P721 with R724; T726 with Q722) that might compromise IFD structure and function and interaction between IFD residues and residues in RT motifs (R811 with D807) or DNA as seen in the cryo-EM structures (20, 21).

TPP1-IFD–interacting residues

Recruitment of telomerase to telomeres is mediated by amino acids in the TPP1 N-terminus known as the TEL patch (TPP1 glutamate [E] and leucine [L] rich) within the oligonucleotide/oligosaccharide-binding (OB) fold and supported by the recent cryo-EM structures (8–10, 20, 21). More recently, another region in the extreme N terminus of the TPP1-OB region (NOB) was also reported to be part of the telomerase interaction surface on TPP1 (38) (Fig. 3*A*). A previous structural homology-based mutagenesis screen described doubly mutated IFD residues V790/I792 and E793/Q794 as important for the localization of hTERT to TPP1 (16). Our current results also support a role for V791 in binding TPP1 (Fig. 2, *D* and *E*). A human TERT-TPP1 homology model was proposed which places the TPP1 NOB domain in close proximity to IFD-TRAP, specifically NOB residues 91-GRLVL-95 and IFD-TRAP residues 790-VVIEQ-794 (16). To determine if the IFD-TRAP residues 790-VVIEQ-794 interact with TPP1 NOB residues 91-GRLVL-95, we introduced the following mutations within the FLAG-hTERT IFD fragment, IFD 790-AAAAA-794 (IFD-5A) and the following mutations within the TPP1-HA NOB region 91-AAAAA-95 (TPP1-5A). We coexpressed either the WT FLAG-hTERT IFD domain or FLAG-hTERT-IFD-5A variant along with either WT TPP1-HA or TPP1-5A-HA in HEK293 cells and confirmed by Western blotting analysis that all the hTERT and TPP1 variants were expressed (Fig. 3*B*). We observed similar levels of coimmunoprecipitated WT TPP1 or TPP1-5A upon IP of either WT IFD or IFD-5A, indicating that disrupting these amino acids in either IFD or TPP1 does not abolish the interaction of IFD with TPP1 (Fig. 3, *B* and *C*). Recent structural studies revealed that TPP1 NOB residues L93 and V94 interact with IFD residues L798 and N799 (Fig. 3*D*) (21). While L93 and V94 are mutated in the TPP1-5A variant that we tested, TPP1 NOB residues S90 and R92, which the structures reveal are interacting with TEN residues L123 and P124 (Fig. 3*D*), were not mutated.

The IFD is not essential for the interaction of the core hTERT domain with the TEN domain

The cryo-EM structure of *Tetrahymena* telomerase reveals that both the TPP1 ortholog p50 and the TEN domain can interact with the IFD-TRAP (14). The authors suggested that p50 may stabilize the IFD-TRAP fold and/or the IFD–TRAP interaction with TEN. To investigate the interaction of the IFD with TEN, we used a transcomplementation approach that has shown that coexpression of an N-terminal hTERT fragment containing TEN (or the TEN domain alone) and another fragment containing the remainder of the hTERT (core) can reconstitute telomerase activity and function (12, 39–41). Based on the *Tetrahymena* telomerase structural data, we expected that deletion variants that lack the TEN domain but contain the IFD (Fig. 1*A*) would interact with the TEN domain. We coexpressed FLAG-hTERT variants ΔTEN, ΔTENΔCTE or IFD region alone with an HA-tagged TEN domain alone (HA-TEN) (residues 1-316) in HEK293 cells and confirmed by Western blotting analysis that all the FLAG-hTERT variants and HA-TEN domain were expressed (Fig. 4*A*). We found that IP of the FLAG-hTERTΔTEN core domain, the ΔTENΔCTE and the IFD domain alone coimmunoprecipitate coexpressed HA-TEN, demonstrating that the IFD interacts with TEN, consistent with the cryo-EM structures of *Tetrahymena* and human telomerase (14, 20–22). However, FLAG-hTERTΔTENΔCTE lacking the IFD (ΔTENΔCTEΔIFD) was still able to coimmunoprecipitate HA-TEN (Fig. 4*A*), suggesting that the IFD is not essential for the interaction with TEN. In addition, these results imply that there may be additional contacts between hTERT and TEN that fall outside of the IFD domain, possibly indirectly mediated through TEN contacts with the telomerase RNA as shown by the cryo-EM structures (14, 20–22). To address this latter possibility, we expressed FL FLAG-hTERT, FLAG-hTERTΔTENΔCTE lacking the IFD (ΔTENΔCTEΔIFD), and FLAG-IFD in HEK293 cells and confirmed by Western blot analysis that all the FLAG-hTERT WT and variants were expressed (Fig. 4*B*). We found that IP of FLAG-hTERT and FLAG-hTERTΔTENΔCTEΔIFD, but not the IFD domain alone, could coimmunoprecipitate hTR as detected by qRT-PCR (Fig. 4, *B* and *C*), though the low binding of the IFD to hTR similar to the EV control did not reach statistical significance. These results are consistent with the idea that additional contacts between hTERT and TEN that

expressing TPP1-HA but transfected with an empty vector not expressing any hTERT variant. Mock represents untransfected HEK293 cells expressing neither hTERT nor TPP1. n = 2. *C*, the mean ratio of $(HA/FLAG)_{IP}$ signal over $((HA/FLAG)/actin)_{Input}$ obtained from quantification with ImageQuant of two independent experiments from panel *B*. *D*, interactions of FLAG-hTERT-IFD and the indicated IFD variants within FLAG-hTERT-IFD with TPP1-HA were assessed by coimmunoprecipitation from HEK293 cell lysates using an anti-FLAG antibody. Representative immunoblots showing input FLAG-hTERT-IFD, the indicated IFD variants and TPP1-HA, and immunoprecipitation of FLAG-hTERT-IFD variants and TPP1-HA. Blots were probed using antibodies against FLAG or HA or the loading control actin (in the input). EV represents HEK293 cells expressing TPP1-HA but transfected with an empty vector not expressing any hTERT variant. Mock represents untransfected HEK293 cells expressing neither hTERT nor TPP1. n = 3. *E*, the mean ratio of $(HA/FLAG)_{IP}$ signal over $((HA/FLAG)/actin)_{Input}$ obtained from quantification with ImageQuant of three independent experiments from panel *D*; error bars represent SD. ANOVA with a Dunnet's multiple comparison with WT as reference: $*p < 0.05$; $****p < 0.0001$. No *p* value indicates quantification was statistically not significant. *F*, human telomerase structure showing where V791, L805, V763, and P785 (represented as *gray spheres*) in the IFD (*purple*) are in relation to TPP1 (*light purple*). hTERT motif 3 in *red* and hTERT TEN in *light blue* are also indicated. Based on PDB: 7QXS. hTERT, human telomerase RT; IFD, insertion in fingers domain; IP, immunoprecipitation; TEN, telomerase essential N-terminal domain.

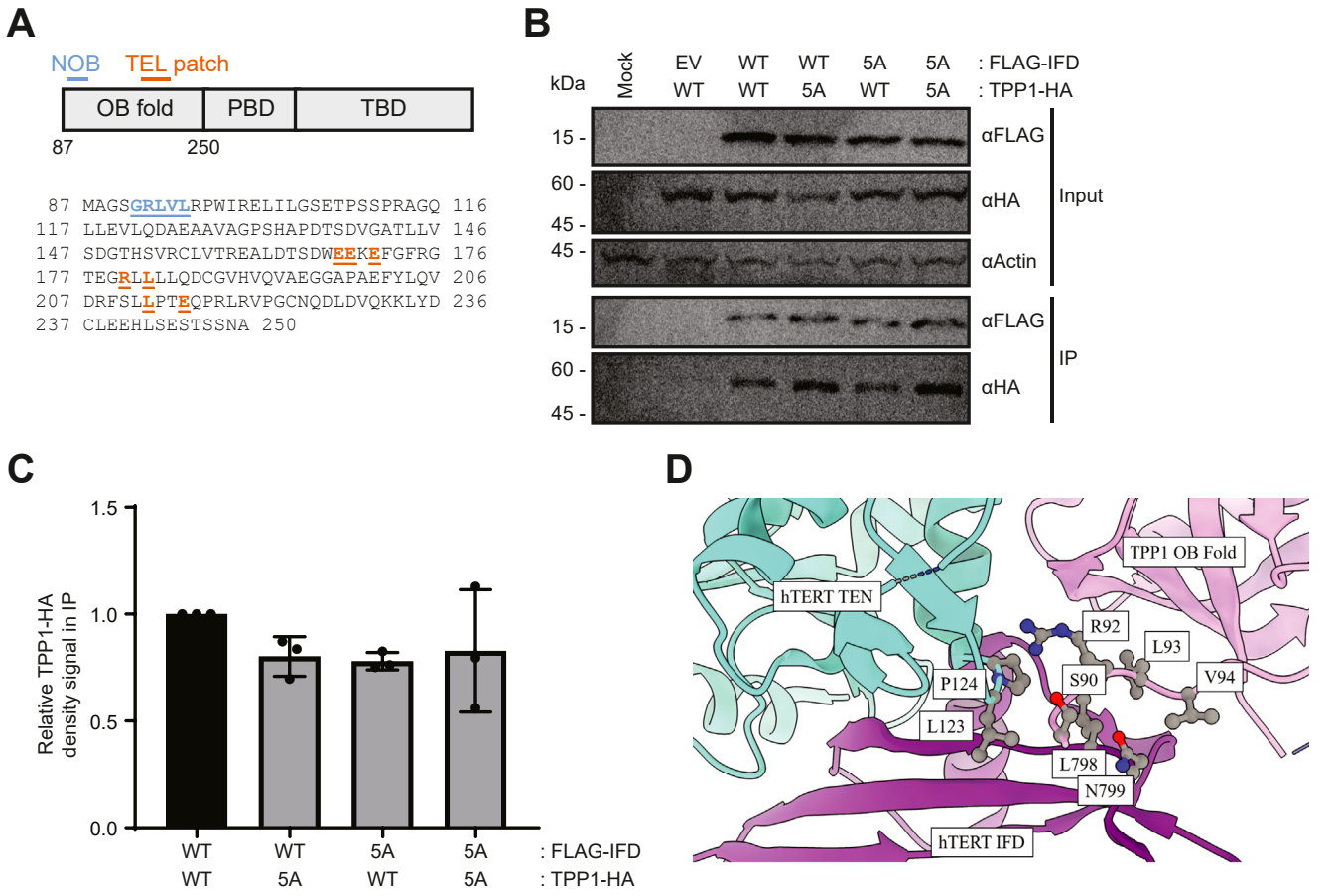

Figure 3. TPP1-IFD interacting residues. *A*, domain organization of human TPP1 with characteristic domains: Oligonucleotide/oligosaccharide binding (OB) fold, shelterin POT1 binding domain (PBD), and a C-terminal domain containing the shelterin TIN2-binding domain (TBD). The sequence of the OB-fold domain is indicated and includes the TEL patch in *orange* important for binding the TEN domain and recruitment of telomerase to telomeres, and the NOB domain in *light blue*, which is part of the telomerase interaction surface on TPP1. *B*, interactions of FLAG-hTERT-IFD and the FLAG-hTERT IFD 790-VVIEQ-794 (IFD-5A) variant with TPP1-HA or the TPP1 91-GRLVL-95 (TPP1-5A) variant were assessed by coimmunoprecipitation from HEK293 cell lysates using an anti-FLAG antibody. Representative immunoblots showing input FLAG-hTERT-IFD, the IFD-5A variant, TPP1-HA, and the TPP1-5A variant, and immunoprecipitation of FLAG-IFD and TPP1-HA. Blots were probed using antibodies against FLAG or HA or the loading control actin (in the input). EV represents HEK293 cells expressing TPP1-HA but transfected with an empty vector not expressing any hTERT variant. Mock represents untransfected HEK293 cells expressing neither hTERT nor TPP1. n = 3. *C*, the mean ratio of $(HA/FLAG)_{IP}$ signal over $((HA/FLAG)/actin)_{Input}$ obtained from quantification with ImageQuant of three independent experiments from panel B.; error bars represent SD. ANOVA with a Dunnet's multiple comparison with WT as reference. No *p* value indicates quantification was statistically not significant. *D*, Human telomerase structure highlighting TPP1 NOB L93 and V94 interacting with IFD L798 and N799 and NOB S90 and R92 interacting with TEN L123 and P124. IFD is in *purple*, TPP1 in *light purple*, and TEN in *light blue*. Based on PDB: 7QXS. hTERT, human telomerase RT; IFD, insertion in fingers domain; IP, immunoprecipitation; NOB, N terminus of the TPP1-OB region; TEN, telomerase essential N-terminal domain.

fall outside the IFD domain may be mediated by the telomerase RNA.

Mapping the IFD–TEN interaction

One of the human TEN regions that maps to the TEN-TRAP interface based on the cryo-EM structure of *Tetrahymena* telomerase falls within human TEN amino acids 161-171 (14). Integration of bioinformatics analysis data with the structure of *Tetrahymena* telomerase allowed the generation of a pseudoatomic model of the human telomerase catalytic core (42). In this model, an extended β-sheet (β14 in the IFD-TRAP and β6 in the TEN domains of *Tetrahymena* telomerase) is formed such that the human IFD region containing residues 786-799 are predicted to interact with the human TEN region containing residues 165-173. From the 2021 human telomerase cryo-EM structure, we identified three potential points of interaction between the human TEN and IFD domains, IFD R756-TEN Y176, IFD R742-TEN Y168, and IFD Q781/D788-TEN S165 (Fig. 5*A*) (19). To determine if these residues are important for the IFD–TEN interaction, we initially introduced mutations in IFD and TEN that would affect each of the three predicted interactions independently. We coexpressed the IFD and TEN variants to test each of the three interactions independently but found no defects in the interaction between IFD and TEN, possibly indicative of compensation from the other points of contact (not shown). We then introduced the following mutations in the IFD, R742A/R756A/Q781A/D788A (RRQD/AAAA) and the following mutations within the TEN region, S165A/Y168A/Y176A (SYY/AAA) to potentially interfere with all three points of contact simultaneously. We coexpressed either the WT

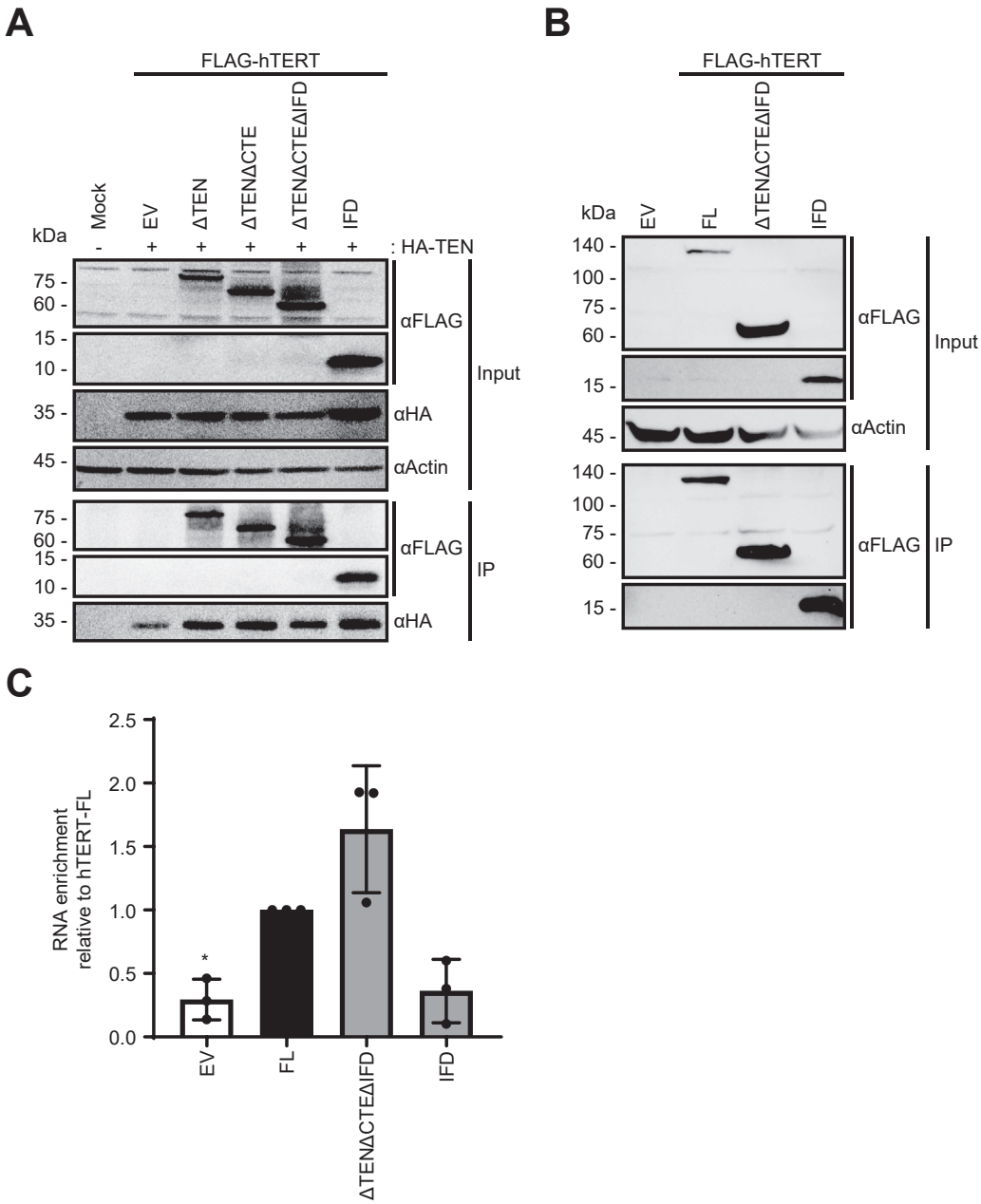

Figure 4. The IFD is not essential for the interaction of the core hTERT domain with the TEN domain. *A*, interactions of FLAG-hTERT WT and the indicated deletion variants with HA-TEN were assessed by coimmunoprecipitation from HEK293 cell lysates using an anti-FLAG antibody. Representative immunoblots showing input FLAG-hTERT WT and variants and HA-TEN, and immunoprecipitation of FLAG-hTERT WT and variants and HA-TEN. Blots were probed using antibodies against FLAG or HA or the loading control actin (in the input). EV represents HEK293 cells expressing HA-TEN but transfected with an empty vector not expressing any hTERT variant. Mock represents untransfected HEK293 cells expressing neither hTERT nor TEN. n = 4. *B*, full length (FL) FLAG-hTERT WT, FLAG-hTERTΔTENΔCTE lacking the IFD (ΔTENΔCTEΔIFD), and FLAG-IFD were immunoprecipitated from HEK293 cell lysates using an anti-FLAG antibody. Representative immunoblots showing input and immunoprecipitated FLAG-hTERT WT, FLAG-hTERTΔTENΔCTEΔIFD, and FLAG-IFD. Blots were probed using antibodies against FLAG or the loading control actin (in the input). EV represents HEK293 cells transfected with an empty vector not expressing any hTERT variant. n = 3. *C*, the mean ratio of RNA enrichment of hTR after FLAG-IP of FLAG-hTERT WT, FLAG-hTERTΔTENΔCTEΔIFD, and FLAG-IFD obtained from the quantification by quantitative real-time polymerase chain reaction of three independent experiments from panel B using the comparative ΔΔ*Ct* method; error bars represent SD. ANOVA with a Dunnet's multiple comparison with WT (FL) as reference. *$p < 0.05$ No *p* value indicates quantification was statistically not significant. hTERT, human telomerase RT; hTR, human telomerase RNA; IFD, insertion in fingers domain; IP, immunoprecipitation; TEN, telomerase essential N-terminal domain.

FLAG-hTERT IFD domain or the FLAG-hTERT-IFD-RRQD/AAAA variant along with either WT HA-TEN or HA-TEN-SYY/AAA variant in HEK293 cells and confirmed by Western blotting analysis that all the IFD and TEN variants were expressed (Fig. 5*B*). Multiple amino acid mutations in the IFD did not abolish the interaction with HA-TEN nor did multiple mutations in the TEN domain abolish interaction with FLAG-IFD, as we observed coimmunoprecipitated HA-TEN or HA-TEN SYY/AAA with either WT FLAG-IFD or FLAG-IFD RRQD/AAAA (Fig. 5, *B* and *C*), suggesting that these amino acid alterations are not sufficient to abolish the interaction between the IFD and TEN. These results also suggest that the

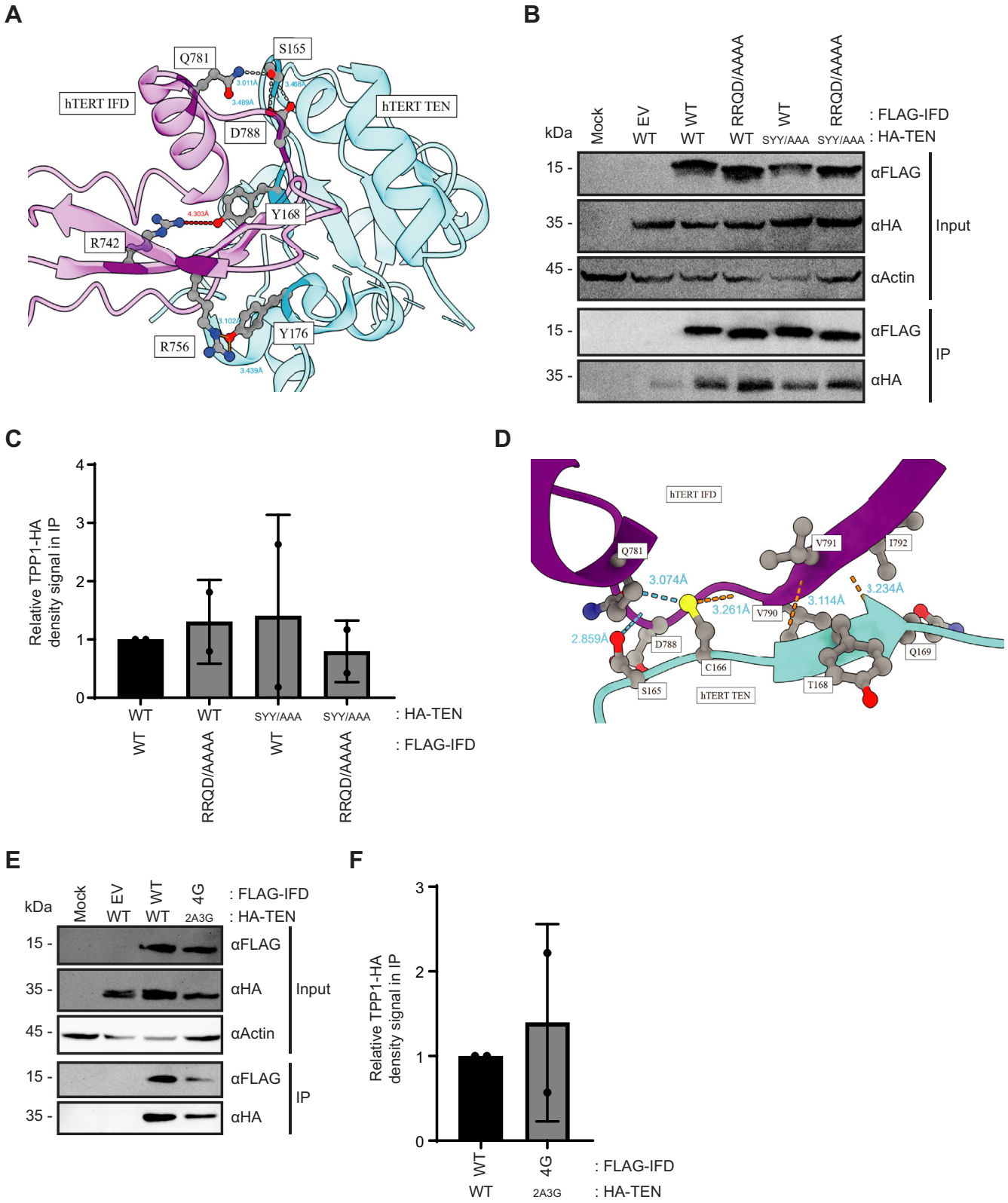

Figure 5. Mapping the IFD-TEN interaction. *A*, human telomerase structure highlighting interactions of IFD R756-TEN Y176, IFD R742-TEN Y168, and IFDQ781/D788-TEN S165. TEN is in *light blue* and IFD is in *purple*. Based on PDB: 7BG9. *B*, interactions of FLAG-hTERT-IFD and the FLAG-hTERT IFD R742A/R756A/Q781A/D788A (RRQD/AAAA) variant with HA-TEN or the S165A/Y168A/Y176A (SYY/AAA) variant were assessed by coimmunoprecipitation from HEK293 cell lysates using an anti-FLAG antibody. Representative immunoblots showing input FLAG-hTERT-IFD, the IFD-RRQD/AAAA variant, HA-TEN, and the TEN-SYY/AAA variant, and immunoprecipitation of FLAG-IFD and HA-TEN. Blots were probed using antibodies against FLAG or HA or the loading control actin (in the input). EV represents HEK293 cells expressing HA-TEN but transfected with an empty vector not expressing any hTERT variant. Mock represents untransfected HEK293 cells expressing neither hTERT nor TEN. n = 2. *C*, the mean ratio of $(HA/FLAG)_{IP}$ signal over $((HA/FLAG)/actin)_{Input}$ obtained from quantification with ImageQuant of two independent experiments from panel *B*. *D*, human telomerase structure showing interaction of IFD 790VVIE793 and

interaction between TEN and IFD may be more stable than between the IFD and TPP1.

More recent 2022 cryo-EM structures of human telomerase with TPP1 and POT1 revealed an IFD β-sheet-TEN β-sheet interface (β6 in TEN and β18 in IFD-TRAP) with interactions between IFD 790VVIE793 and TEN 167AYQ169. Interactions between IFD residues D788 and TEN S165 and between IFD residues Q781 and TEN C166 were also observed (Fig. 5*D*). To disrupt the β-sheet interface and investigate if the TEN S165 and C166 residues are important for the IFD–TEN interaction, we introduced the following mutations in the IFD 790-VVIE-793 to 790-GGGG-793 (IFD-4G) and the following mutations within the TEN region, 165-SCAYQ-169 to 165-AAGGG-169 (TEN-2A3G). In an effort to better disrupt the β-sheet interface, we mutated those residues to glycine rather than alanine (43). We coexpressed either the WT FLAG-hTERT IFD domain or the FLAG-hTERT-IFD-4G variant along with either WT HA-TEN or HA-TEN-2A3G variant in HEK293 cells and confirmed by Western blotting analysis that all the IFD and TEN variants were expressed (Fig. 5*E*). Multiple amino acid mutations in the IFD and in the TEN domain did not abolish the interaction between the IFD and TEN as we observed coimmunoprecipitated HA-TEN-2A3G with FLAG-IFD-4G (Fig. 5, *E* and *F*), suggesting that these amino acid alterations are not sufficient to abolish the interaction between the IFD and TEN.

In conclusion, our data suggest that the IFD interacts with both TPP1 and the TEN domain, but the IFD is not essential for hTERT's interaction with either TPP1 or TEN. Several conserved residues in the central IFD-TRAP region that we reported regulate telomerase recruitment to telomeres and, cell immortalization compromise interaction of the hTERT-IFD domain with TPP1 when mutated. The recent cryo-EM structures provide context to published biochemical and functional data. However, the published structures also reveal networks of complex interactions between the IFD, TEN, and TPP1 that may be necessary to provide flexibility in coordinating nucleic acid–protein interactions. Our results suggest that these extensive, multiple and coordinated interactions may compensate for the disruption of certain pairwise interactions that possibly occur during telomere synthesis. Further structural studies examining intermediate stages in telomere synthesis may help to understand the biochemical and molecular defects of mutant telomerase enzymes and would be of primary importance for the design of therapeutic treatments.

Experimental procedures

Cell culture and transfection

HEK293 cells were maintained in Dulbecco's modified Eagle's Medium (Wisent) supplemented with 10% fetal bovine serum (Wisent) and antibiotics/antimycotics (Gibco). Transfection was performed with Lipofectamine 2000 (Invitrogen) according to manufacturer's instructions. Transfection reagent and DNA were mixed in Opti-MEM media (Gibco) and overlaid on cells in Dulbecco's modified Eagle's Medium with 10% fetal bovine serum, then changed to regular media 5 h posttransfection.

Plasmid constructs and cloning

N-terminal 3xFLAG-c-myc-NLS-hTERT truncations were cloned downstream and in-frame of a FLAG tag between NheI and HindIII of pcDNA3.1-N3xFLAG. c-myc-NLS refers to the c-myc NLS previously used to target proteins to the nucleus (44). C-terminal HA-tagged TPP1 and N-terminal HA-tagged hTERT (TEN) were cloned into pcDNA3.1(+) Hygro between NheI and HindIII. TPP1 was C-terminally tagged since N-terminally tagging TPP1 has been reported to impair TPP1 regulation of telomerase function (45). For truncations with the deleted IFD motif, the full plasmid was amplified with 5′-phosphorylated (T4 PNK; NEB) primers omitting the IFD sequence and purified on a G-25 column (GE). The amplified fragment was ligated with T4 ligase (Life Technologies) overnight at room temperature and then transformed into DH5α *Escherichia coli* cells. To generate IFD variants, site-directed mutagenesis was conducted on hTERT truncation plasmids with the *Pfu* Turbo polymerase (Agilent) according to manufacturer instructions (all primers used for cloning and mutagenesis are listed in Table 1).

Coimmunoprecipitation

A previously published protocol (8) was adapted for FLAG co-IP of FLAG-NLS-hTERT truncations and TPP1-HA. Briefly, transfected HEK293 cells were washed with ice-cold PBS 1× and then suspended in 250 μl of 2× lysis buffer (50 mM Tris pH 7.4, 20% glycerol, 1 mM EDTA, 150 mM NaCl, 0.5% Triton X-100, 0.02% SDS, 1 mM DTT + 1 mM PMSF + 2× protease inhibitor cocktail (Sigma)). After 5 min on ice, 12.5 μl of 5 M NaCl was added and further incubated on ice for 5 min. Lysate was centrifuged at max speed (13,000 RPM) after addition of 263 μl of ice-cold water. Cell lysate was precleared with 40 μl of prewashed slurry Sepharose protein G beads (GE) for 1 h on rotator at 4 °C. Beads were pelleted at 2400 RPM, and cell lysate was quantified with Bradford reagent (Bio-Rad). Input was prepared using 50 μg of protein mixed with Laemmli. Immunoprecipitation was performed with an equal amount of protein between samples and FLAG antibody (Sigma #F7425) was added. After 2 h of incubation at 4 °C on rotator, 40 μl of prewashed slurry Sepharose protein G beads was added and incubated for 1 h. Three 5-min wash

TEN 167AYQ169 within the IFD β-sheet-TEN β-sheet interface (β18 in IFD-TRAP and β6 in TEN) and interactions between IFD residues D788 and TEN S165, and between IFD residues Q781 and TEN C166. Based on PDB: 7QXS. *E*, interactions of FLAG-hTERT-IFD and the FLAG-hTERT IFD 790VVIE/4G variant with HA-TEN or the TEN 167SCAYQ/2A3G variant were assessed by coimmunoprecipitation from HEK293 cell lysates using an anti-FLAG antibody. Representative immunoblots showing input FLAG-hTERT-IFD, the IFD-VVIE/4G variant, HA-TEN, and the TEN-167SCAYQ/2A3G variant, and immunoprecipitation of FLAG-IFD and HA-TEN. Blots were probed using antibodies against FLAG or HA or the loading control actin (in the input). EV represents HEK293 cells expressing HA-TEN but transfected with an empty vector not expressing any hTERT variant. Mock represents untransfected HEK293 cells expressing neither hTERT nor TEN. n = 2. *F*, the mean ratio of $(HA/FLAG)_{IP}$ signal over $((HA/FLAG)/actin)_{Input}$ obtained from quantification with ImageQuant of two independent experiments from panel *E*. hTERT, human telomerase RT; IFD, insertion in fingers domain; IP, immunoprecipitation; TEN, telomerase essential N-terminal domain.

Table 1
Primers (P) used for cloning the different TEN, IFD, TPP1 sequences encoding variant domains and proteins

hTERT variant	P	Primer sequence
ΔTEN	F	GGGGCTAGCACCTGCTGCCAAGAGGGTCAAGTTGGACTGGGACACGCCTTGT
	R	CCCAAGCTTTCAGTCCAGGATGGTC
ΔTENΔCTE	F	GGGGCTAGCACCTGCTGCCAAGAGGGTCAAGTTGGACTGGGACACGCCTTGT
	R	CCCAAGCTTTTACAGCAGCAGGCCG
IFD fragment	F	GGGGCTAGCACCTGCTGCCAAGAGGGTCAAGTTGGACCCCCAGGACAGGC
	R	CCCAAGCTTTTAGCACATGAAGCGTAGG
ΔTENΔCTEΔIFD	F	CACCACGCCGTGC
	R	GATGGTGTCGTACGCG
P721R	F	GGTCAAGTTGGACCTAGCTCGCCAGGACAGGCTCACGGAGG
	R	CCTCCGTGAGCCTGTCCTGGCGAGCTAGGT CCAACTTGACC
T726M	F	CCAGGACAGGCTCATGGAGGTCATCGCCAG
	R	CTGGCGATGACCTCCATGAGCCTGTCCTGG
V763S	F	GGCCTTCAAGAGCCACAGCTCTACCTTGACAGAC
	R	GTCTGTCAAGGTAGAGCTGTGGCTCTTGAAGGCC
P785L	F	GGAGACCAGCCTGCTGAGGGATGCCG
	R	CGGCATCCCTCAGCAGGCTGGTCTCC
V791Y	F	CTGAGGGATGCCGTCTACATCGAGCAGAGCTC
	R	GAGCTCTGCTCGATGTAGACGGCATCCCTC
L805A	F	CAGCAGTGGCGCCTTCGACGTCTTCCTACG
	R	GACGTCGAAGGCGCCACTGCTGGCCTCATTC
R811C	F	CTTCGACGTCTTCCTATGCTTCATGTGCCACC
	R	GGTGGCACATGAAGCATAGGAAGACGTCGAAG
IFD(5A)	F	GACCAGCCCGCTGAGGGATGCCGCTGCTGCTGCTAGCTCCTCCCTGAATGAGGCC
	R	GGCCTCATTCAGGGAGGAGCTAGCAGCAGCAGCAGCGGCATCCCTCAGCGGGCTGGTC
IFD(R742A)	F	CAGAACACGTACTGCGTGGCTCGGTATGCCGTGGTCCAG
	R	CTGGACCACGGCATACCGAGCCACGCAGTACGTGTTCTG
IFD(R756A)	F	GCCGCCCATGGGCACGTCGCCAAGGCCTTCAAGAGCCAC
	R	GTGGCTCTTGAAGGCCTTGGCGACGTGCCCATGGGCGGC
Q781A	F	CAGTTCGTGGCTCACCTGGCGGAGACCAGCCCGCTGAG
	R	CTCAGCGGGCTGGTCTCCGCCAGGTGAGCCACGAACTG
D788A	F	GAGACCAGCCCGCTGAGGGCTGCCGTCGTCATCGAGCAG
	R	CTGCTCGATGACGACGGCAGCCCTCAGCGGGCTGGTCTC
IFD(4G)	F	CTGCAGGAGACCAGCCCGCTGAGGGATGCCGGGGGAGGA GGGCAGAGCTCCTCCCTGAATGAGGCCAGCAGT
	R	ACTGCTGGCCTCATTCAGGGAGGAGCTCTGCCCTCCTCCC CCGGCATCCCTCAGCGGGCTGGTCTCCTGCAG
TPP1-HA	F	GTAAGCTAGCATGGCAGGTTCGGGG
	R	CCCAAGCTTTTAAGCGTAATCTGGAACATCGTATGGGTACATCGGAGTTGGCTCAGA
TPP1(5A)	F	CAAGCTGGCTAGCATGGCAGGTTCGGCTGCTGCTGCTGCTCGGCCCTGGATTCGGGAG
	R	GAATCAGCTCCCGAATCCAGGGCCGAGCAGCAGCAGCAGCCGAACCTGCCATGCTAGC
HA-TEN	F	GGGGCTAGCATGTACCCATACGATGTTCCAGATTACGCTCCGCGCGCTCC
	R	CCCAAGCTTTTAACGTGGTGGCCG
TEN(S165A)	F	CTTTGTGCTGGTGGCTCCCGCCTGCGCCTACCAGGTGTGC
	R	GCACACCTGGTAGGCGCAGGCGGGAGCCACCAGCACAAAG
TEN(Y168A)	F	GTGGCTCCCGCCTGCGCCGCCCAGGTGTGCGGGCCGCCG
	R	CGGCGGCCCGCACACCTGGGCGGCGCAGGCGGGAGCCAC
TEN(Y176A)	F	GTGTGCGGGCCGCCGCTGGCCCAGCTCGGCGCTGCCACTC
	R	GAGTGGCAGCGCCGAGCTGGGCCAGCGGCGGCCCGCACAC
TEN(2A3G)	F	GCACGCTGCGCGCTCTTTGTGCTGGTGGCTCCCGCTGCC GGGGGAGGGGTGTGCGGGCCGCCGCTGTACCAGCTCGGCGCT
	R	AGCGCCGAGCTGGTACAGCGGCGGCCCGCACACCCCTCCCCC GGCAGCGGGAGCCACCAGCACAAAGAGCGCGCAGCGTGC

Underline indicates the sequence of the HA tag.
F, forward primer. R, reverse primer.

cycles were performed with 1× lysis buffer on rotator at 4 °C. Pelleted beads were suspended in 60 μl Laemmli 1× prior to boiling, and 30 μl was loaded on gel for analysis. Co-IP of FLAG-NLS-hTERT(IFD) variants and TPP1-HA was performed the same way.

FLAG co-IP of FLAG-NLS-hTERT truncations and HA-hTERT(TEN) was adapted from a previous publication (12). Briefly, transfected HEK293 cells were washed with ice-cold PBS 1× and then suspended in 250 μl HLB buffer (20 mM Hepes pH 8.0, 2 mM $MgCl_2$, 10% glycerol, 0.2 mM EGTA, 0.1% IGEPAL, 1 mM DTT + 1 mM PMSF + 1× protease inhibitor cocktail). Cells were lysed with 3 freeze-thaw cycles followed by addition of 21.7 μl of 5 M NaCl. Cell lysate was collected after centrifugation at max speed (13,000 RPM) and then precleared by adding 40 μl of prewashed slurry Sepharose protein G beads for 1 h at 4 °C on rotator. Beads were pelleted and cell lysate was quantified with Bradford reagent. For input, 50 μg of protein was mixed with Laemmli and an equal amount of protein was immunoprecipitated with FLAG antibody (Sigma #F7425). After 2 h incubation on rotor at 4 °C, 40 μl of prewashed slurry Sepharose protein G beads was added and incubated on rotator for 1 h at 4 °C. Three cycles of washes were performed with HLB supplemented with 150 mM NaCl, 0.1% Triton X-100, and 0.2% Chaps on rotator for 5 min at room temperature. Beads were centrifuged and suspended in 80 μl Laemmli 1× and then boiled. Forty microliters were loaded on gel for analysis. Co-IP of FLAG-NLS-hTERT(IFD) variants and HA-hTERT(TEN) was performed the same way.

Immunoprecipitation and qRT-PCR

FLAG co-IP of FLAG-NLS-hTERT truncations coupled to quantitative real-time polymerase chain reaction (qPCR) of

hTR was performed as previously described (46). Briefly, transfected HEK293 cells were washed with ice-cold PBS 1× and then suspended in 150 µl low-salt cytosolic lysis buffer (25 mM Hepes pH 7.9, 0.5 mM $MgCl_2$, 5 mM KCl, 0.5% NP-40 + 1× protease inhibitor + 0.04 U/µl RNaseOUT (Life Technologies)). After 10 min on ice, cells were centrifuged at 3000 RPM, and the cytosolic fraction was transferred into a fresh tube and kept on ice. Pellet was suspended in 150 µl high-salt nuclear lysis buffer (25 mM Hepes pH 7.9, 10% sucrose, 350 mM NaCl, 0.01% NP-40 + 1× protease inhibitor + 0.04 U/µl RNaseOUT) and incubated on rotator at 4 °C for 30 min. Both cytosolic and nuclear fraction were pooled, centrifuged at max speed (13,000 RPM) for 30 min, and cell lysate was incubated for 30 min at 4 °C with 40 µl of prewashed slurry Sepharose protein G beads. Beads were pelleted at 2400 RPM, and cell lysate was quantified with Bradford reagent. Input for Western blotting was prepared using 50 µg of protein mixed with Laemmli, whereas input for qPCR was prepared using a quantity of protein representing 10% of the IP mixed into 500 µl TRIzol (Life Technologies) and kept at −80 °C until RNA extraction. IP was performed with an equal amount of protein between samples and FLAG antibody (Sigma #F3165). After 2 h on rotator at 4 °C, 40 µl of prewashed Sepharose protein G beads slurry was added and incubated for 1 h. Beads were washed 3 times with modified radioimmunoprecipitation assay buffer (50 mM Tris pH 8.0, 150 mM NaCl, 10 mM $MgCl_2$, 1% NP-40, 0.5% sodium deoxycholate + 1 mM PMSF + 1× protease inhibitor + 0.02 U/µl RNaseOUT). Half of pelleted beads were suspended in 60 µl Laemmli 1×, boiled and 30 µl was loaded on gel for analysis. Rest of pelleted beads were suspended into 500 µl TRIzol and kept at −80 °C until RNA extraction which was performed according to reagent instructions. Both SuperScript II RT cDNA synthesis and PerfCTa SYBR green FastMix with Low ROX (Quantabio) qPCR were performed according to manufacturer instructions. qPCR was performed in a 7500Fast Real-Time PCR system (Applied Biosystem) and the comparative $\Delta\Delta C_T$ method was applied to analyze RNA enrichment between samples.

Immunoblotting

Immunoblot was performed with standard protocol for these antibodies used at specified dilution: mouse anti-actin (Cell Signaling Technology #3700, 1:5000), mouse anti-HA (Cell Signaling Technology #2367, 1:1250), rabbit anti-FLAG (Proteintech #20543-1-AP, 1: 4000). PVDF membrane (Millipore) was blocked with fat-free skim milk in PBS-Tween 0.1% or TBS-Tween 0.1% followed by blotting with primary antibody overnight at 4 °C. Membrane was washed three times and then blotted with secondary antibody (HRP-conjugated mouse anti-rabbit (Sigma) or rabbit anti-mouse (Sigma), 1:10,000) for 1 h at room temperature. Signal was revealed with ECL Plus substrate (Thermo Fisher Scientific) after 3 washes.

Immunofluorescence

Coverslips from transfected HEK293 cells were transferred from a 60 mm dish to a 6-well plate for immunofluorescence. Remaining cells in dish were lysed on ice in TRAP lysis buffer (10 mM Tris pH 7.5, 1 mM $MgCl_2$, 1 mM EGTA, 10% glycerol, 150 mM NaCl, 5 µM β-mercaptoethanol, 0.1% IGEPAL + 1 mM PMSF + protease inhibitor) and analyzed by Western blotting for protein expression. Coverslips were washed with PBS 1× and then cells were fixed with 4% formaldehyde in PBS 1× for 10 min at room temperature. After a quick wash with 1× PBS, cells were permeabilized with 0.1% Triton X-100 in 1× PBS for 5 min at 4 °C. Cells were rehydrated with 50% formamide in 2× SSC (30 mM $Na_3C_6H_5O_7$ pH 7.0, 300 mM NaCl) for 5 min at room temperature and then washed three times with 1× PBS for 10 min at room temperature on a rocking platform. Cells were blocked with 3% bovine serum albumin in PBS-Tween 0.1% for 1 h at room temperature in a humid chamber and then primary rabbit anti-FLAG antibody (Sigma #F7425; 1:500 in PBG (1% cold fish gelatin, 0.1% bovine serum albumin in 1× PBS)) was added and incubated overnight at 4 °C in a humid chamber. After three washes with PBS-Tween 0.1% for 5 min on a rocking platform, cells were incubated with Cy3-labeled donkey anti-rabbit (Jackson ImmunoResearch Lab Inc., 1:125 in PBG) for 1 h at room temperature in a humid chamber. Cells were further washed three times with 1× PBS for 5 min at room temperature on a rocking platform and then mounted in an anti-fading agent containing DAPI (Vector Laboratories). Images were captured by LSM800 confocal microscope provided by the Core Facility at the Lady Davis Institute, at 63× magnification using the ZEN Pro software (https://www.zeiss.com/microscopy/en/products/software/zeiss-zen.html).

Quantification

The mean ratio of $(HA/FLAG)_{IP}$ signal over $((HA/FLAG)/actin)_{Input}$ obtained from quantification with ImageQuant of at least two independent experiments was performed as in (47). Statistical analysis was performed using ANOVA with a Dunnet's multiple comparison with WT as reference.

Data availability

All data are contained in the article or available on request by contacting the corresponding author: chantal.autexier@mcgill.ca.

Acknowledgments—We thank Alexandre Garus and Jian Qin for discussion and comments on the manuscript. We also thank Kelly Nguyen for discussion and sharing data prior to publication.

Author contributions—P. L. L., A. Y., and C. A. conceptualization; P. L. L. and A. Y. methodology; P. L. L., A. Y., and C. A. formal analysis; P. L. L. and A. Y. investigation; P. L. L. and A. Y. writing–review and editing; P. L. L. and A. Y. visualization; A. Y. validation; C. A. resources; C. A. writing–original draft; C. A. supervision; C. A. project administration; C. A. funding acquisition.

Funding and additional information—Financial support was provided from Canadian Institute for Health Research Grant PJT-166130 to C. A. Support to A. Y. was provided by a McGill

University Faculty of Medicine Internal Studentship and Fonds de la Recherche Québec-Santé doctoral award.

Conflict of interest—The authors declare that they have no conflicts of interest with the contents of this article.

Abbreviations—The abbreviations used are: CTE, C-terminal extension; FL, full length; hTERT, human telomerase RT; hTR, human telomerase RNA; IFD, insertion in fingers domain; IP, immunoprecipitation; NLS, nuclear localization signal; NOB, N terminus of the TPP1-OB region; OB, oligosaccharide-binding; RT, reverse transcriptase; TEN, telomerase essential N-terminal domain.

References

1. Jafri, M. A., Ansari, S. A., Alqahtani, M. H., and Shay, J. W. (2016) Roles of telomeres and telomerase in cancer, and advances in telomerase-targeted therapies. *Genome Med.* **8**, 69
2. Armanios, M. (2022) The role of telomeres in human disease. *Annu. Rev. Genomics Hum. Genet.* **23**, 363–381
3. Bertuch, A. A. (2016) The molecular genetics of the telomere biology disorders. *RNA Biol.* **13**, 696–706
4. Townsley, D. M., Dumitriu, B., and Young, N. S. (2014) Bone marrow failure and the telomeropathies. *Blood* **124**, 2775–2783
5. Autexier, C., and Lue, N. (2006) The structure and function of telomerase reverse transcriptase. *Annu. Rev Biochem* **75**, 493–517
6. Wu, R. A., Upton, H. E., Vogan, J. M., and Collins, K. (2017) Telomerase mechanism of telomere synthesis. *Annu. Rev. Biochem.* **86**, 439–460
7. Schmidt, J. C., and Cech, T. R. (2015) Human telomerase: biogenesis, trafficking, recruitment, and activation. *Genes Dev.* **29**, 1095–1105
8. Nandakumar, J., Bell, C. F., Weidenfeld, I., Zaug, A. J., Leinwand, L. A., and Cech, T. R. (2012) The TEL patch of telomere protein TPP1 mediates telomerase recruitment and processivity. *Nature* **492**, 285–289
9. Sexton, A. N., Youmans, D. T., and Collins, K. (2012) Specificity requirements for human telomere protein interaction with telomerase holoenzyme. *J. Biol. Chem.* **287**, 34455–34464
10. Zhong, F. L., Batista, L. F., Freund, A., Pech, M. F., Venteicher, A. S., and Artandi, S. E. (2012) TPP1 OB-fold domain controls telomere maintenance by recruiting telomerase to chromosome ends. *Cell* **150**, 481–494
11. Chu, T. W., D'Souza, Y., and Autexier, C. (2016) The insertion in fingers domain in human telomerase can mediate enzyme processivity and telomerase recruitment to telomeres in a TPP1-dependent manner. *Mol. Cell Biol.* **36**, 210–222
12. Robart, A. R., and Collins, K. (2011) Human telomerase domain interactions capture DNA for TEN domain-dependent processive elongation. *Mol. Cell* **42**, 308–318
13. Wu, R. A., and Collins, K. (2014) Human telomerase specialization for repeat synthesis by unique handling of primer-template duplex. *EMBO J.* **33**, 921–935
14. Jiang, J., Wang, Y., Sušac, L., Chan, H., Basu, R., Zhou, Z. H., *et al.* (2018) Structure of telomerase with telomeric DNA. *Cell* **173**, 1179–1190.e13
15. Xie, M., Podlevsky, J. D., Qi, X., Bley, C. J., and Chen, J. J. (2010) A novel motif in telomerase reverse transcriptase regulates telomere repeat addition rate and processivity. *Nucl. Acids Res* **38**, 1982–1996
16. Tesmer, V. M., Smith, E. M., Danciu, O., Padmanaban, S., and Nandakumar, J. (2019) Combining conservation and species-specific differences to determine how human telomerase binds telomeres. *Proc. Natl. Acad. Sci. U. S. A.* **116**, 26505–26515
17. Chu, T. W., MacNeil, D. E., and Autexier, C. (2016) Multiple mechanisms contribute to the cell growth defects imparted by human telomerase insertion in fingers domain mutations associated with premature aging diseases. *J. Biol. Chem.* **291**, 8374–8386
18. Jiang, J., Chan, H., Cash, D. D., Miracco, E. J., Ogorzalek Loo, R. R., Upton, H. E., *et al.* (2015) Structure of Tetrahymena telomerase reveals previously unknown subunits, functions, and interactions. *Science* **350**, aab4070
19. Ghanim, G. E., Fountain, A. J., van Roon, A. M., Rangan, R., Das, R., Collins, K., *et al.* (2021) Structure of human telomerase holoenzyme with bound telomeric DNA. *Nature* **593**, 449–453
20. Liu, B., He, Y., Wang, Y., Song, H., Zhou, Z. H., and Feigon, J. (2022) Structure of active human telomerase with telomere shelterin protein TPP1. *Nature* **604**, 578–583
21. Sekne, Z., Ghanim, G. E., van Roon, A. M., and Nguyen, T. H. D. (2022) Structural basis of human telomerase recruitment by TPP1-POT1. *Science* **375**, 1173–1176
22. Wan, F., Ding, Y., Zhang, Y., Wu, Z., Li, S., Yang, L., *et al.* (2021) Zipper head mechanism of telomere synthesis by human telomerase. *Cell Res.* **31**, 1275–1290
23. Armbruster, B. N., Etheridge, K. T., Broccoli, D., and Counter, C. M. (2003) Putative telomere-recruiting domain in the catalytic subunit of human telomerase. *Mol. Cell. Biol.* **23**, 3237–3246
24. Banik, S. S. R., Guo, C., Smith, A. C., Margolis, S. S., Richardson, D. A., Tirado, C. A., *et al.* (2002) C-terminal regions of the human telomerase catalytic subunit essential for *in vivo* enzyme activity. *Mol. Cell. Biol.* **22**, 6234–6246
25. Sealey, D. C., Zheng, L., Taboski, M. A., Cruickshank, J., Ikura, M., and Harrington, L. A. (2010) The N-terminus of hTERT contains a DNA-binding domain and is required for telomerase activity and cellular immortalization. *Nucl. Acids Res.* **38**, 2019–2035
26. [preprint] Evans, R., O'Neill, M., Pritzel, A., Antropova, N., Senior, A., Green, T., *et al.* (2022) Protein complex prediction with AlphaFold-Multimer. *bioRxiv*. https://doi.org/10.1101/2021.10.04.463034
27. Mirdita, M., Schütze, K., Moriwaki, Y., Heo, L., Ovchinnikov, S., and Steinegger, M. (2022) ColabFold: making protein folding accessible to all. *Nat. Met.* **19**, 679–682
28. Jumper, J., Evans, R., Pritzel, A., Green, T., Figurnov, M., Ronneberger, O., *et al.* (2021) Highly accurate protein structure prediction with AlphaFold. *Nature* **596**, 583–589
29. Varadi, M., Anyango, S., Deshpande, M., Nair, S., Natassia, C., Yordanova, G., *et al.* (2022) AlphaFold protein structure database: massively expanding the structural coverage of protein-sequence space with high-accuracy models. *Nucl. Acids Res* **50**, D439–D444
30. D'Souza, Y., Chu, T. W., and Autexier, C. (2013) A translocation-defective telomerase with low levels of activity and processivity stabilizes short telomeres and confers immortalization. *Mol. Biol. Cell* **24**, 1469–1479
31. Collins, K., and Greider, C. W. (1993) Tetrahymena telomerase catalyzes nucleolytic cleavage and non-processive elongation. *Genes Dev.* **7**, 1364–1376
32. Harrington, L. A., and Greider, C. W. (1991) Telomerase primer specificity and chromosome healing. *Nature* **353**, 451–454
33. Jacobs, S. A., Podell, E. R., and Cech, T. R. (2006) Crystal structure of the essential N-terminal domain of telomerase reverse transcriptase. *Nat. Struct. Mol. Biol.* **13**, 218–225
34. Lee, M. S., and Blackburn, E. H. (1993) Sequence-specific DNA primer effects on telomerase polymerization activity. *Mol. Cell. Biol.* **13**, 6586–6599
35. Morin, G. B. (1991) Recognition of a chromosome truncation site associated with alpha-thalassaemia by human telomerase. *Nature* **353**, 454–456
36. Romi, E., Baran, N., Gantman, M., Shmoish, M., Min, B., Collins, K., *et al.* (2007) High-resolution physical and functional mapping of the template adjacent DNA binding site in catalytically active telomerase. *Proc. Natl. Acad. Sci. U. S. A.* **104**, 8791–8796
37. Wu, R. A., Tam, J., and Collins, K. (2017) DNA-binding determinants and cellular thresholds for human telomerase repeat addition processivity. *EMBO J.* **36**, 1908–1927
38. Grill, S., Tesmer, V. M., and Nandakumar, J. (2018) The N terminus of the OB domain of telomere protein TPP1 is critical for telomerase action. *Cell Rep.* **22**, 1132–1140
39. Beattie, T. L., Zhou, W., Robinson, M. O., and Harrington, L. (2000) Polymerization defects within human telomerase are distinct

from telomerase RNA and Tep1 binding. *Mol. Biol. Cell* **11**, 3329–3340
40. Beattie, T. L., Zhou, W., Robinson, M. O., and Harrington, L. (2001) Functional multimerization of the human telomerase reverse transcriptase. *Mol. Cell. Biol.* **21**, 6151–6160
41. Moriarty, T. J., Marie-Egyptienne, D. T., and Autexier, C. (2004) Functional organization of repeat addition processivity and DNA synthesis determinants in the human telomerase multimer. *Mol. Cell. Biol.* **24**, 3720–3733
42. Wang, Y., Gallagher-Jones, M., Sušac, L., Song, H., and Feigon, J. (2020) A structurally conserved human and tetrahymena telomerase catalytic core. *Proc. Natl. Acad. Sci. U. S. A.* **117**, 31078–31087
43. Merkel, J. S., and Regan, L. (1998) Aromatic rescue of glycine in beta sheets. *Fold Des* **3**, 449–455
44. Ray, M., Tang, R., Jiang, Z., and Rotello, V. M. (2015) Quantitative tracking of protein trafficking to the nucleus using cytosolic protein delivery by nanoparticle-stabilized nanocapsules. *Bioconjug. Chem.* **26**, 1004–1007
45. Sandhu, R., Wei, D., Sharma, M., and Xu, L. (2019) An N-terminal Flag-tag impairs TPP1 regulation of telomerase function. *Biochem. Biophys. Res. Commun.* **512**, 230–235
46. MacNeil, D. E., Lambert-Lanteigne, P., Qin, J., McManus, F. P., Bonneil, E., Thibault, P., *et al.* (2021) SUMOylation- and GAR1-dependent regulation of dyskerin nuclear and subnuclear localization. *Mol. Cell Biol.* **41**, e00464-20
47. Burckhardt, C. J., Minna, J. D., and Danuser, G. (2021) Co-immunoprecipitation and semi-quantitative immunoblotting for the analysis of protein-protein interactions. *STAR Protoc.* **2**, 100644